

Paramagnetic Effect in Superconductors. I. Theoretical Aspects*

HANS MEISSNER

Department of Physics, Johns Hopkins University, Baltimore, Maryland

(Received December 14, 1954)

A theory for the paramagnetic effect is developed under the assumption that the ratio of the effective length to the effective diameter l/a of the superconducting particles in the transition region is constant. While experiment shows that the relative apparent permeability \tilde{K}_m is a function of $\gamma = \varphi_0(1 - I_g/I)$, where $\varphi_0 = H_{\varphi 0}/H_{z 0}$, $H_{\varphi 0}$ is the circular and $H_{z 0}$ the longitudinal component of the field at the surface, I_g is a limiting current, and I the total current through the sample, this theory gives the permeability as a function of φ_0 only. Good agreement with the experimental range of \tilde{K}_m , however, is obtained when the theoretical value of φ_0 is replaced by γ . The experiments of the author *et al.* on solid and hollow mercury cylinders and recent experiments of Thompson and Squire on a solid tin cylinder are discussed. A reason why the theoretical value of φ_0 has to be replaced by γ cannot be given at this time, although it is indicated where the present theory has to be amended.

I. INTRODUCTION

WHEN a large direct current is passed longitudinally through a long cylindrical superconductor in the presence of a weak longitudinal magnetic field while the temperature is lowered through the transition region, Steiner¹ found that the longitudinal flux inside the cylinder may exceed that in the normal-conducting state. This flux increase occurs only if the current exceeds a certain minimum value.

It was proven² that this "paramagnetic effect" is due to a helical path of the current through the superconductor. Recently Teasdale and Rorschach³ and Thompson and Squire⁴ confirmed the existence of the paramagnetic effect. The following points were considered in II to develop a working model of the superconductor in this particular state: The temperature dependence of the resistance is in qualitative agreement with the calculations of London⁵ on the transition of a cylindrical superconductor in which a current is flowing (compare Fig. 3 in II and Fig. 41 in reference 5). At the point of maximum flux (and we are so far only interested in this point of the flux *vs* temperature curve) the total magnetic field at the surface of the superconductor is equal to the critical field H_c . According to London's theory the superconductor consists of superconducting particles embedded in normal-conducting material. If only the current is present, then the magnetic field has only a circular component $H_{\varphi} = H_c$ and the shape of the superconducting particles could be the one suggested by Shoenberg (see reference 5, page 120, Fig. 40). If a longitudinal magnetic field is now superimposed, H_z inside the superconductor will

be larger than zero and the superconducting particles will have the shape of "propellers" or of grains oriented along a helix.

In both cases a helical path offers less resistance to the current than a straight one. The current will flow along a helix and will produce an additional longitudinal flux inside the superconductor.

Defining an apparent relative permeability (denoted by $\tilde{\mu}$ in II):

$$\tilde{K}_m = \frac{1}{R^2 \pi \mu_0 H_{z 0}} \int_0^R 2\pi r B_z(r) dr, \quad (1)$$

[R = radius of superconductor, $B_z(r)$ = z -component of the macroscopic magnetic induction, $H_{z 0}$ = external magnetic field, μ_0 = permeability of vacuum], it was shown that the current necessary to reach $\tilde{K}_m = 1$, i.e., the value of the normal conductor, is given by:

$$I(\tilde{K}_m = 1) = I_g + \gamma 2\pi R H_{z 0}, \quad (2)$$

where the observed values of I_g and γ are listed in Table I. Solving Eq. (2) for γ and noting that $I = 2\pi R H_{\varphi 0}$ (we use the rationalized mks-system), we find

$$\gamma = \frac{H_{\varphi 0}}{H_{z 0}} \left(1 - \frac{I_g}{I} \right). \quad (2')$$

We consider γ now as a variable, which has the values listed in Table I at $\tilde{K}_m = 1$. In Fig. 1(a), measurements of \tilde{K}_m for mercury are plotted as a function of γ (compare II Fig. 4, where \tilde{K}_m is plotted as a function of I).

TABLE I. Observed values of the characteristics constants I_g and γ for various superconductors.*

Atomic number	Element	Transition temperatures	Limiting current I_g amp	Factor γ
49	In	3.4	0.6	0.67
50	Sn	3.6	1.2	0.67
73	Ta	4.3	0.6	?
80	Hg	4.2	1.7	0.37
81	Tl	2.4	0.6	0.37

* γ is given for R in m, $H_{z 0}$ in amp/m.

* Supported by a grant of the National Science Foundation.

¹ K. Steiner and H. Schoeneck, *Physik. Z.* **38**, 887 (1937). K. Steiner, *Z. Naturforsch.* **4a**, 271 (1949).

² Meissner, Schmeissner, and Meissner, *Z. Physik* **130**, 521 (1951); **130**, 529 (1951); **132**, 529 (1952) referred to in the text as I, II, and III; *Phys. Rev.* **90**, 709 (1953).

³ T. S. Teasdale and H. E. Rorschach, Jr., *Phys. Rev.* **90**, 709 (1953).

⁴ J. C. Thompson and C. F. Squire, *Phys. Rev.* **96**, 287 (1954).

⁵ F. London, *Superfluids* (Wiley & Sons, New York, 1950), Vol. 1, p. 120.

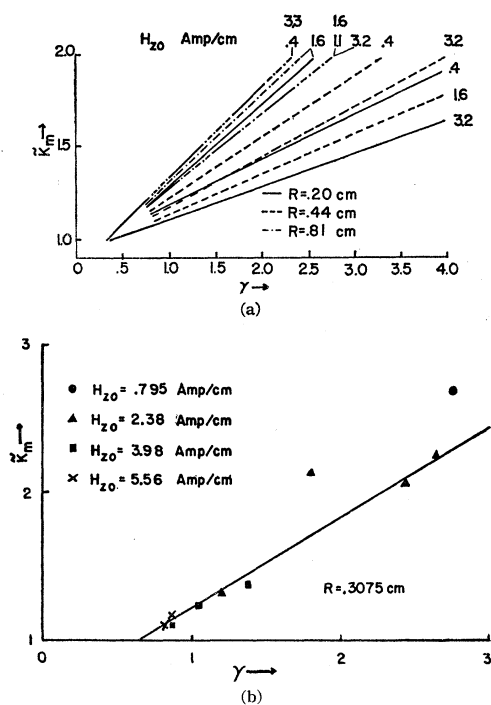


FIG. 1. (a) Relative permeability \tilde{K}_m vs γ for different solid mercury cylinders and different values of the external field. Note that some of the curves coincide, so that 6 of the 11 measured curves are very close together. All curves are recalculated from the original measurements. (b) Relative permeability \tilde{K}_m vs γ for a solid tin cylinder (from measurements of Thompson and Squire).

In Fig. 1(b), measurements for tin are plotted in the same fashion (compare Fig. 4 of reference 3, where $\tilde{B} - \mu_0 H_{z0}$ is plotted as function of I). Higher values of γ correspond to higher currents. The plots show that there is no obvious dependence of the curves either on the diameter of the sample or on the external magnetic field, although the curves for mercury scatter very much. We conclude therefore that \tilde{K}_m depends only on γ :

$$\tilde{K}_m = \tilde{K}_m(\gamma) = \tilde{K}_m[\varphi_0(1 - I_g/I)], \quad (3)$$

where $\varphi_0 = H_{\varphi_0}/H_{z0}$. The experimental scattering range of γ apparently increases with \tilde{K}_m and is very small for $\tilde{K}_m = 1$.

It will be shown in the following section that by simple additions to the London theory of the current-carrying superconductor we can obtain a paramagnetic effect. In this theory, however, \tilde{K}_m depends on φ_0 only:

$$\tilde{K}_m = \tilde{K}_m(\varphi_0). \quad (4)$$

Furthermore it will be shown that, although Eq. (4) differs from Eq. (3), we get the right scattering range if we simply replace γ by φ_0 .

II. THEORY OF THE PARAMAGNETIC EFFECT IN SOLID CYLINDERS

We choose a layer between r and $r + dr$ in our superconductor and stretch it out to a plane. The

superconducting grains (or the cross sections of the superconducting "propellers") will give a pattern indicated in Fig. 2. We choose the Z -axis parallel to the original one and the Y -axis parallel to the former φ direction. The spacing between the superconducting particles will be rather uniform, so that the local value of the magnetic field is always $h = H_c$. The direction of the particles is determined by the magnetic field since the force of the electric field is too small to move the boundaries appreciably.

We define the macroscopic magnetic induction \mathbf{B} in the following way: We choose a plane whose normal vector \mathbf{f} is parallel to \mathbf{B} , so that

$$\mathbf{B} \cdot \mathbf{f} = \mu_0 \int \mathbf{h} \cdot d\mathbf{f}.$$

Since $|\mathbf{h}| = H_c$, this gives approximately

$$\mathbf{B} = \mu_0 \xi_{II} \mathbf{H}, \quad \text{with } \xi_{II} = d/(a+d), \quad (5)$$

where a/d is the ratio of the thickness of the particles to the spacing between the particles. \mathbf{H} has the magnitude H_c and the direction of the mean value of the local field \mathbf{h} . Since \mathbf{H} has both components H_z and H_y , the vector \mathbf{B} will make an angle α with the y -axis.

We choose now a set of axes η, ζ such that η is parallel to \mathbf{B} and ζ is perpendicular to \mathbf{B} .

If we apply an electric field \mathbf{E}_ζ in the ζ direction, calling e_ζ the local value of the electric field, we find for the mean value:

$$\zeta E_\zeta = \int e_\zeta d\zeta,$$

or, since e_ζ is fairly constant,

$$E_\zeta = \xi_{II} e_\zeta. \quad (6)$$

If we apply an electric field \mathbf{E}_η in the η direction, then

$$\eta E_\eta = \int e_\eta d\eta,$$

and, by the same reasoning as above,

$$E_\eta = \xi_{II} e_\eta, \quad \text{with } \xi_{II} = d/(l+d), \quad (7)$$

where l/d is the ratio of the length of the particles to the spacing between particles.

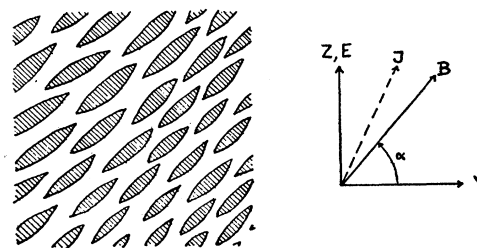


FIG. 2. Layer of superconducting particles (shaded) oriented in the direction of the magnetic induction B .

For an electric field in any other direction, we suppose that we can use with fair accuracy the ordinary transformation scheme; this means that we suppose the superposition principle to hold for the macroscopic fields E_η and E_ζ . We get then for instance:

$$E_z = E_\eta \sin\alpha + E_\zeta \cos\alpha, \quad E_y = E_\eta \cos\alpha - E_\zeta \sin\alpha.$$

The current density J is given by

$$J_\zeta = \sigma_n e_\zeta, \quad J_\eta = \sigma_n e_\eta,$$

where σ_n is the value of the conductivity for the normal-conducting material.

Since $E_y = E_\varphi = 0$ we find then for the current density, using Eq. (6) and (7):

$$\begin{aligned} J_y &= (\sigma_I - \sigma_{II}) \sin\alpha \cos\alpha E_z, \\ J_z &= (\sigma_I \sin^2\alpha + \sigma_{II} \cos^2\alpha) E_z, \end{aligned} \quad (8)$$

where

$$\sigma_I = \sigma_n / \xi_I, \quad \sigma_{II} = \sigma_n / \xi_{II} \quad (9)$$

are the principal values of the macroscopic anisotropic conductivity. If the angle α is zero, the equations reduce to London's equations (reference 5).

It follows from Eq. (5) that $\xi_{II} = B / \mu_0 H_c = d / (a + d)$, which, together with Eq. (7) and (9), gives

$$\frac{\sigma_I}{\sigma_{II}} - 1 = \left(\frac{l}{a} - 1 \right) \left(1 - \frac{B}{\mu_0 H_c} \right) = C \left(1 - \frac{B}{\mu_0 H_c} \right), \quad (10)$$

where $C = l/a - 1$ may be still a function of the radius. Noting that

$$\sin\alpha = H_z / H_c, \quad \cos\alpha = H_y / H_c, \quad (11)$$

we find, using Eq. (10), that

$$\begin{aligned} J_y &= \frac{\mu_0 H_c}{B} C \left(1 - \frac{B}{\mu_0 H_c} \right) \frac{H_y H_z}{H_c^2} \sigma_n E_z, \\ J_z &= \frac{\mu_0 H_c}{B} \left[C \left(1 - \frac{B}{\mu_0 H_c} \right) \frac{H_z^2}{H_c^2} + 1 \right] \sigma_n E_z. \end{aligned} \quad (12)$$

For $H_z = 0$ these equations reduce again to the appropriate equations given by London.

We now return to cylindrical coordinates:

$$J_z \rightarrow J_z, \quad J_y \rightarrow J_\varphi, \quad \dots$$

We note that \mathbf{H} is not a function of z and that $H_r = 0$. The expression for $\text{curl}\mathbf{H}$ then reduces to

$$\text{curl}_z \mathbf{H} = \frac{1}{r} \frac{\partial(rH_\varphi)}{\partial r}, \quad \text{curl}_r \mathbf{H} = 0, \quad \text{curl}_\varphi \mathbf{H} = -\frac{\partial H_z}{\partial r}. \quad (13)$$

We have further

$$H_y^2 + H_z^2 = H_c^2. \quad (14)$$

The Maxwell equation $\text{curl}\mathbf{H} = \mathbf{J}$ then becomes

$$\frac{1}{r} \frac{\partial(rH_\varphi)}{\partial r} = J_z, \quad -\frac{\partial H_z}{\partial r} = J_\varphi. \quad (15)$$

From Eqs. (14) and (15), we obtain

$$H_z J_\varphi / H_\varphi + H_\varphi / r = J_z.$$

Using Eq. (12) and solving for B , we find

$$B = \mu_0 H_c \sigma_n E_z r / H_\varphi. \quad (16)$$

At the surface of the superconductor, $r = R$, the induction B has the value $B = \mu_0 H_c$ and $H_\varphi = H_{\varphi 0}$. Thus

$$R = H_{\varphi 0} / \sigma_n E_z \quad (17)$$

and

$$B = \mu_0 H_c r H_{\varphi 0} / R H_\varphi. \quad (18)$$

For $H_{z0} = 0$ we have $H_{\varphi 0} = H_c$ and the equations revert to London's corresponding equations.

The mean relative permeability \bar{K}_m is now given by

$$\bar{K}_m = \frac{1}{\pi R^2} \int_0^R \frac{H_z H_{\varphi 0} r}{H_{z0} H_\varphi R} 2\pi r dr. \quad (19)$$

In order to obtain the dependence of \mathbf{H} on r , we have to solve Eq. (15) with the aid of Eqs. (12), (14), (17), and (18). We obtain

$$\frac{dH_\varphi}{dr} = C \left(\frac{H_\varphi}{r} - \frac{H_{\varphi 0}}{R} \right) \left(1 - \frac{H_\varphi^2}{H_c^2} \right), \quad (20)$$

where $C = l/a - 1$ may be a function of r . Similarly, we obtain

$$-\frac{dH_z}{dr} = C \left(\frac{(H_c^2 - H_z^2)^{\frac{1}{2}}}{r} - \frac{H_{\varphi 0}}{R} \right) \frac{H_z (H_c^2 - H_z^2)^{\frac{1}{2}}}{H_c^2}. \quad (21)$$

Since the superconducting particles have always the same field H_c around them, we will now assume that C is constant, independent of r .

Then as $r \rightarrow 0$ Eq. (20) becomes:

$$\lim_{r \rightarrow 0} \left(r \frac{dH_\varphi}{dr} \right) = C H_\varphi(0) \left(1 - \frac{H_\varphi^2(0)}{H_c^2} \right).$$

It can be shown that this equation has only the following, physically significant, solutions: Either $H_\varphi(0) = 0$ or $H_\varphi(0) = H_c$. We know from the calculations of F. London that the latter solution holds for the case $H_{z0} = 0$. One concludes that even a small field H_{z0} changes the pattern of the superconducting particles entirely, so that now $H_\varphi(0) = 0$ and $H_z(0) = H_c$.

For numerical calculations we put Eqs. (20) and (21) in a dimensionless form. With

$$\begin{aligned} \varphi &= H_\varphi / H_{z0}; \quad \chi = H_z / H_{z0}; \quad \rho = r / R; \\ H_c / H_{z0} &= (1 + \varphi_0^2)^{\frac{1}{2}}, \end{aligned} \quad (22)$$

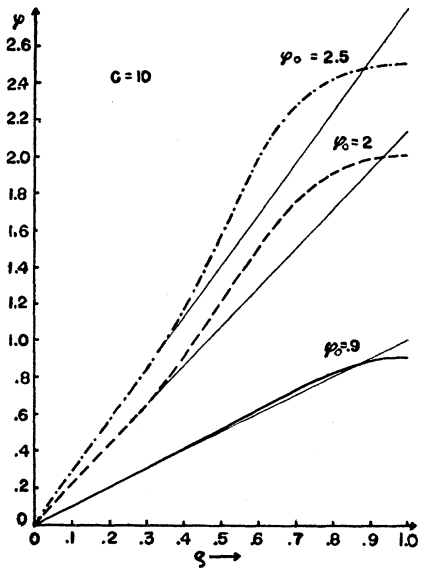
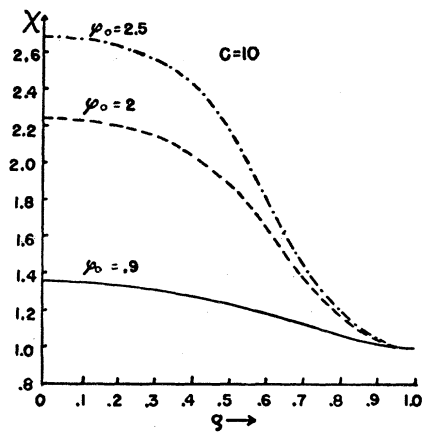


FIG. 3. Circular (upper figure) and longitudinal (lower figure) component of the magnetic field vs radius for different values of φ_0 . φ_0 is the circular component of the field at the surface of the sample. It is proportional to the total current. All curves for $C=10$. Thin lines: $\varphi = \varphi_0 \rho / (C-1)$.

we obtain:

$$\frac{d\varphi}{d\rho} = C \left(\frac{\varphi}{\rho} - \varphi_0 \right) \left(1 - \frac{\varphi^2}{1 + \varphi_0^2} \right), \quad (20')$$

$$\frac{d\chi}{d\rho} = C \left(\frac{[1 - \chi^2 / (1 + \varphi_0^2)]^{\frac{1}{2}}}{\rho} \frac{\varphi_0}{(1 + \varphi_0^2)^{\frac{1}{2}}} \right) \times \chi [1 - \chi^2 / (1 + \varphi_0^2)]^{\frac{1}{2}}, \quad (21')$$

$$\bar{K}_m = \frac{1}{\pi} \int_0^1 \frac{\varphi_0}{\varphi} - \rho \chi 2\pi \rho d\rho. \quad (19')$$

\bar{K}_m is a function of φ_0 only. This is exactly what we have stated in Eq. (4).

Equations (20') and (21') cannot be solved in analytical form. We have solved one of them by numerical methods for $C=10$. The result is plotted in Fig. 3.

It can be shown that

$$\varphi = [C / (C-1)] \varphi_0 \rho \quad (23)$$

is a good approximation for φ . The approximation improves as C increases, or more specifically, if

$$(1 + \varphi_0^2) / \varphi_0^2 \gg C^2 / (C-1)^2.$$

We will use Eq. (23) for the limiting case $C = \infty$, which will not differ very much from the case $C=100$. From the curves in Fig. 3 we can now calculate the local value of K_m :

$$K_m = \rho \chi \varphi_0 / \varphi.$$

The result is plotted in Fig. 4(a). It can be seen that most of the flux increase occurs near the center of the sample. Integrating over r according to Eq. (19') gives

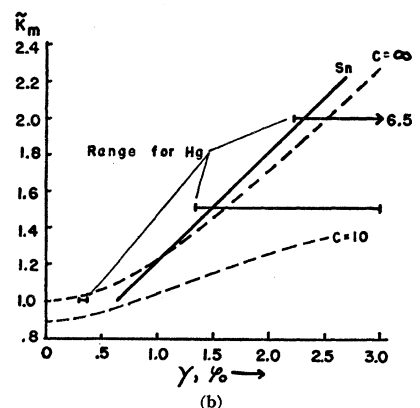
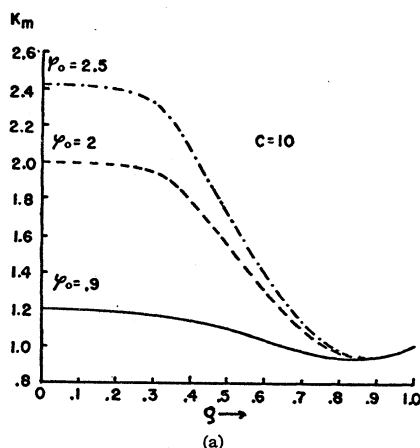


FIG. 4. (a) Local values of the relative permeability K_m vs radius for different values of φ_0 . All curves for $C=10$. (b) Mean values of the relative permeability \bar{K}_m . Broken curves: theoretical values of K_m as function of φ_0 for $C=10$ and $C = \infty$. Solid line: experimental values of \bar{K}_m as function of γ for tin (from measurements of Thompson and Squire). Horizontal lines: experimental scattering range of \bar{K}_m as function of γ for mercury.

the mean value of \bar{K}_m . This is plotted as function of φ_0 in Fig. 4(b). (Broken curve $C=10$.)

With Eq. (23) we can immediately derive an analytical expression for $\bar{K}_m(\varphi_0)$:

$$\bar{K}_m = \frac{2}{3} \varphi_0 \left(1 - \frac{1}{C}\right)^3 \left\{ \left(\frac{1 + \varphi_0^2}{\varphi_0^2}\right)^{\frac{3}{2}} - \left[\frac{1 + \varphi_0^2}{\varphi_0^2} - \left(\frac{1}{1 - 1/C}\right)^2 \right]^{\frac{3}{2}} \right\}. \quad (24)$$

We used Eq. (24) in order to calculate the curve for $C = \infty$ and the part below $\varphi_0 = 0.8$ of the curve for $C = 10$, where Eq. (23) is a good approximation.

We now replace φ_0 by $\gamma = \varphi_0(1 - I_g/I)$ and indicate according to Fig. 1(a) the scattering range of the measurements on mercury by horizontal lines at $\bar{K}_m = 1$, $\bar{K}_m = 1.5$, and $\bar{K}_m = 2$. We see that this range lies approximately between the curve for $C = 10$ and the curve for $C = \infty$ although we would expect a much larger scattering range for $\bar{K}_m = 1$. The scattering arises apparently from a variation in C at different runs. The solid curve represents the measurements of Thompson and Squire on tin according to Fig. 1(b). Since they had only one sample of very high purity, which did not melt between different runs as the mercury did, they observed no scattering.

Summarizing the results on solid cylinders, we can say that although we are unable to show that \bar{K}_m depends on γ rather than only on φ_0 , the numerical values of \bar{K}_m which we expect for a certain current I are rather good.

III. THEORY OF THE PARAMAGNETIC EFFECT IN HOLLOW CYLINDERS

In III, measurements on hollow, current-carrying cylinders in external fields were reported. However, before we discuss the case of current and external field, let us first see what we would expect if only the current I_z flows through the sample.

As in London's theory for the solid cylinder, $H_\varphi = H_c$. The question now arises as to how the field can be

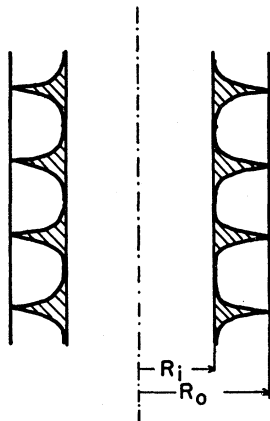


FIG. 5. Cross section through a hollow cylinder in which a current flows in the intermediate state. Superconducting areas shaded.

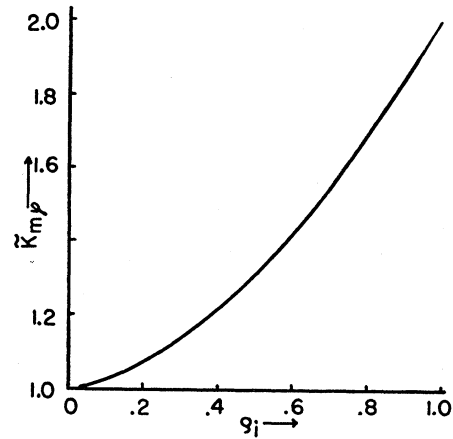


FIG. 6. Increase of the maximum circular flux in the intermediate state relative to the flux in the normal-conducting state as a function of $\rho_i = R_i/R_o$ (theoretical).

equal to H_c near the inner surface $r = R_i$. Apparently, the conical superconducting rings now spread out to a thin layer as indicated in Fig. 5. The limiting current which can pass through a thin layer is smaller than that, which would be calculated from the value of H_c for the bulk material. In other words: For a thin, current-carrying superconducting layer, H_c is smaller than for the bulk material. The thickness of this layer will be of the order of 10^{-4} cm.

For the bulk of the material, $B = B_\varphi$ has the same value as for the solid cylinder:

$$B_\varphi = \mu_0 H_\varphi r / R. \quad (25)$$

Since we can neglect the thin layer, the maximum circular flux per unit length is given by

$$\phi_{\varphi \max} = \int_{R_i}^{R_o} B_\varphi dr = \mu_0 H_c (R_o^2 - R_i^2) / 2R_o. \quad (26)$$

The field distribution in the normal-conducting state is given by

$$H_{\varphi n} = H_{\varphi 0} \frac{R_o}{R_o^2 - R_i^2} \left(r - \frac{R_i^2}{r} \right), \quad (27)$$

and the flux per unit length by

$$\phi_{\varphi n} = \mu_0 H_{\varphi 0} \frac{R_o}{(R_o^2 - R_i^2)} \left[\frac{1}{2} (R_o^2 - R_i^2) - R_i^2 \ln \frac{R_o}{R_i} \right]. \quad (28)$$

Since the total current in the normal-conducting and in the intermediate state is the same, it follows that $H_{\varphi 0} = H_c$.

We define now

$$\bar{K}_{m\varphi} = \frac{\phi_{\varphi \max}}{\phi_{\varphi n}} = \frac{\frac{1}{2} (R_o^2 - R_i^2)^2}{R_o^2 \left[\frac{1}{2} (R_o^2 - R_i^2) - R_i^2 \ln (R_o/R_i) \right]}$$

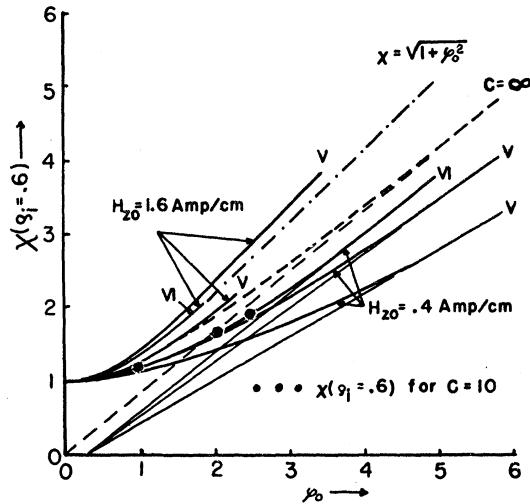


FIG. 7. Field in the hole of hollow cylinders as function of the circular field at the surface of the cylinder for $\rho_i = R_i/R_o = 0.60$. Solid lines: experimental curves for mercury samples V and VI. Dots: theoretical values for $C = 10$. Dashed curve: theoretical values for $C = \infty$. Dot-dashed curve: $\chi = (1 + \varphi_0^2)^{1/2}$ that corresponds to $H_z(\rho_i, \varphi_0) = H_z$.

or in dimensionless form with $\rho_i = R_i/R_o$:

$$\tilde{K}_{m\varphi} = \frac{(1 - \rho_i^2)^2}{(1 - \rho_i^2) + \rho_i^2 \ln \rho_i^2} \quad (29)$$

It follows from Eq. (29) that the flux in the intermediate state is always greater than in the normal state: $2 \geq \tilde{K}_{m\varphi} \geq 1$. $\tilde{K}_{m\varphi}$ depends only on the ratio of the inner to the outer diameter and is independent of the current. In Fig. 6, we have plotted $\tilde{K}_{m\varphi}$ vs ρ_i .

This effect has been reported in the literature⁶ although the authors finally doubted its existence (1939).

Superimposing an additional field H_φ further increases the flux, which Steiner¹ called the transverse paramagnetic effect.

If we superimpose now an external field H_{z0} , we again get the splitting up of the conical rings. Measurements of the increase of the longitudinal flux in the hole and over the whole cross section have been reported (III, Fig. 6). The two mercury samples had the outer radii: sample V: $R_o = 0.4375$ cm, sample VI: $R_o = 0.810$ cm. The ratio of the inner to the outer radius was the same in both cases: $\rho_i = R_i/R_o = 0.60$.

We assume, now, that we have in the bulk material the same distribution of current and field as in a solid cylinder and that we have a thin current layer at the inner surface which brings the field H_φ up to the necessary value.

The field H_z on both sides of this layer will be about the same; i.e., it will have approximately the value which it has at $\rho = \rho_i$ in a solid cylinder.

⁶ K. Steiner, *Physik. Z.* **38**, 880 (1937); Stark, Steiner, and Schoeneck, *Physik. Z.* **38**, 887 (1937); K. Steiner and H. Schoeneck, *Physik. Z.* **40**, 43 (1939).

We now find that the curves of the measurements in the hole come very close together if we plot $\chi(\rho_i, \varphi_0) = H_z(\rho_i, \varphi_0)/H_{z0}$ as a function of $\varphi_0 = H_\varphi/H_{z0}$. This is done in Fig. 7 (solid curves). There is a slight change of the curves with H_{z0} , indicating that the layer still contributes somewhat to the field H_z . From Eq. (14) it follows that

$$\chi(\rho_i, \varphi_0) \leq (1 + \varphi_0^2)^{1/2}, \quad (30)$$

which is generally observed by the measurements. One case, where χ is slightly above the curve $\chi = (1 + \varphi_0^2)^{1/2}$ (the dot-dashed curve) is probably due to a slightly wrong scaling factor in the measurements of χ . If $\chi = (1 + \varphi_0^2)^{1/2}$, then the layer current is zero.

We can now obtain $\chi(\rho_i, \varphi_0)$ for $C = 10$ from our curves in Fig. 3 (dots). If we assume Eq. (23) to hold and choose $C = \infty$, then $\chi(\rho_i, \varphi_0)$ is given by

$$\chi(\rho_i, \varphi_0) = [1 + \varphi_0^2(1 - \rho_i^2)]^{1/2}. \quad (31)$$

This curve is also plotted in Fig. 7 (broken curve). We see that the scattering which we expect on account of a change in C is relatively small. The fact that the curves for higher H_{z0} values are above the $C = \infty$ curve is, as already mentioned, probably due to a contribution of the layer current to H_z .

The asymptote of $\chi(\rho_i, \varphi_0)$ in Eq. (31) is given by

$$\chi_{\text{asympt}} = \varphi_0(1 - \rho_i^2)^{1/2}$$

which intersects the φ_0 -axis at $\varphi_0 = 0$. The asymptotes of the measured curves seem to intersect the φ_0 -axis at $\varphi_0 = 0.25$. However, the measurements are not carried far enough to tell whether this difference is real.

These measurements give one very significant indication: χ is apparently a function of φ_0 rather than of γ . This means our differential equations Eqs. (20) and (21) are probably right and the change from Eq. (4) to Eq. (3) arises out of a change in the expression for B Eq. (18).

The measurements of the flux through the whole cross section of hollow cylinders as functions of the total current have little meaning. The more important quantity is the flux through the ring section. Furthermore we want to plot the flux, or \tilde{K}_m , versus γ rather than versus I .

The first conversion is easy to make. We have:

$$\tilde{K}_{m \text{ ring}} = \frac{R_o^2 \tilde{K}_m(\text{whole sample}) - R_i^2 \chi(\text{hole})}{R_o^2 - R_i^2}. \quad (32)$$

According to Eq. (2'), γ is given by

$$\gamma = \varphi_0(1 - I_0/I);$$

this means by

$$\gamma = \varphi_0 \text{ (correction factor).}$$

We easily find φ_0 from the known values of $H_{\varphi 0}$ and H_{z0} . However, there is some ambiguity as to what value we have to use for this correction factor. Without

special reasoning we will use the following: $I_0=1.7$ amp as for solid mercury cylinders; $I=I_{\text{bulk}}$, the bulk current, that is the total current minus the layer current. The layer current is given by

$$I_{\text{layer}} = 2\pi R_i H_\varphi(\rho_i, \varphi_0),$$

where $H_\varphi(\rho_i, \varphi_0)$ is the value just inside the current layer and may be calculated from

$$H_\varphi(\rho_i, \varphi_0) = H_{z0} [1 + \varphi_0^2 - \chi^2(\text{hole})]^{\frac{1}{2}}.$$

γ is now entirely given by known parameters of the measurements. In Fig. 8, the relative permeability for the ring section is plotted *vs* γ for the two mercury samples V and VI and external field values of $H_{z0}=0.4$ amp/cm and $H_{z0}=1.6$ amp/cm. As for the measurements in the hole of the cylinder, there seems to be a slight dependence on H_{z0} , which may be attributed to the layer current.

In the same way as we did for the solid cylinder, we now identify our theoretical value φ_0 with γ .

Integrating in Fig. 4(a) the local $K_m(\rho)$ between $\rho=\rho_i$ and $\rho=1$, we get $\bar{K}_{m \text{ ring}}(\rho_i, \varphi_0)$ for $C=10$ (lower broken curve in Fig. 8). For the limiting case $C=\infty$, we use Eq. (23) and find, in the same fashion as for the solid cylinder, by integrating, this time from $\rho=\rho_i$ to $\rho=1$,

$$\bar{K}_{m \text{ ring}} = \frac{2}{3} \{ [1 + \varphi_0^2(1 - \rho_i^2)]^{\frac{3}{2}} - 1 \} / \varphi_0^2(1 - \rho_i^2). \quad (37)$$

This curve also is plotted in Fig. 8 (upper broken curve).

We see that the curves for $C=10$ and $C=\infty$ give about the right scattering range for the measured curves.

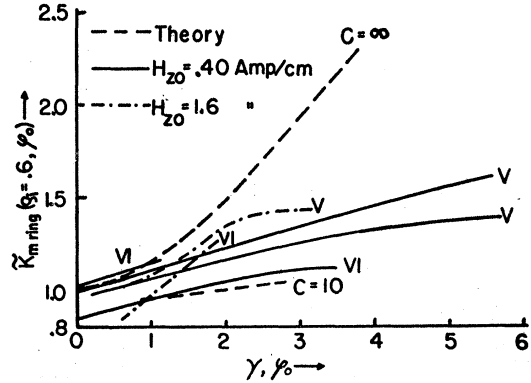


FIG. 8. Increase of the longitudinal flux in the ring section of hollow cylinders. Theoretical curves as function of φ_0 . Experimental curves as function of γ .

VI. CONCLUSIONS

Although we did not end up exactly with the experimental result, it seemed worth while to demonstrate what an extension of the ordinary theory of the current-carrying superconductor would give for the "paramagnetic effect." In this extension essentially only one new assumption was made: It was assumed that the shape of the superconducting particles is independent of the radius. This was made plausible by pointing out that the local field around the particles is always the critical field.

It seems that essentially new concepts are necessary in order to bring the theory into exact agreement with the experiment. Only these new concepts will bring the explanation of the "magic constants" I_0 .

The author wishes to thank the National Science Foundation for supporting this work by a grant.